

This work has only studied non-channel-coded PNC systems. Going forward, the study of channel-coded PNC under the multipath fading scenario will be interesting. In addition, investigation of PNC via a large-delay multipath fading channel is also worthwhile.

REFERENCES

- [1] S. Zhang, S. C. Liew, and P. P. Lam, "Hot topic: Physical-layer network coding," in *Proc. ACM MOBICOM*, 2006, pp. 358–365.
- [2] L. Lu, S. C. Liew, and S. Zhang, "Optimal decoding algorithm for asynchronous physical-layer network coding," in *Proc. IEEE ICC*, Jun. 2011, pp. 1–6.
- [3] L. Lu and S. C. Liew, "Asynchronous physical-layer network coding," *IEEE Trans. Wireless Commun.*, vol. 11, no. 2, pp. 819–831, Feb. 2012.
- [4] S. Zhang, S. C. Liew, and H. Wang, "Synchronization analysis in physical layer network coding, Dec. 2009. [Online]. Available: <http://arxiv.org/ftp/arxiv/papers/1001/1001.0069.pdf>
- [5] U. Bhat and T. M. Duman, "Decoding strategies for physical-layer network coding over frequency selective channels," in *Proc. IEEE Wireless Commun. Netw. Conf.*, Apr. 2012, pp. 12–17.
- [6] F. Rossetto and M. Zorzi, "A practical architecture for OFDM-based decode-and-forward physical-layer network coding," *IEEE Trans. Signal Process.*, vol. 60, no. 9, pp. 4747–4757, Sep. 2012.
- [7] L. Lu, T. Wang, S. C. Liew, and S. Zhang, "Implementation of physical-layer network coding," *Phys. Commun.*, vol. 6, no. 1, pp. 74–87, Mar. 2013.
- [8] X. Xia, K. Xu, and Y. Xu, "Asynchronous physical-layer network coding scheme for two-way OFDM relay, Apr. 2012. [Online]. Available: <http://arxiv.org/abs/1204.2692>
- [9] L. Lu, L. You, and S. C. Liew, "Network-coded multiple access," *IEEE Trans. Mobile Comput.*, to be published.
- [10] *Guidelines for Evaluation of Radio Transmission Technologies for IMT-2000*, ITU-R Std. Recommendation M.1225, 1997.
- [11] M. Zhang, L. Lu, and S. C. Liew, "An optimal decoding strategy for physical-layer network coding over multipath fading channels, Feb. 2014. [Online]. Available: <http://arxiv.org/abs/1402.6882>, Tech. Rep.
- [12] F. R. Kschischang, B. J. Frey, and H.-A. Loeliger, "Factor graphs and the sum-product algorithm," *IEEE Trans. Inf. Theory*, vol. 47, no. 2, pp. 498–519, Feb. 2001.
- [13] S. Verdú, *Multuser Detection*. Cambridge, U.K.: Cambridge Univ. Press, 1998.

A Practical Semidynamic Clustering Scheme Using Affinity Propagation in Cooperative Picocells

Haijun Zhang, *Member, IEEE*, Hui Liu,
Chunxiao Jiang, *Member, IEEE*, Xiaoli Chu, *Member, IEEE*,
A. Nallanathan, *Senior Member, IEEE*, and Xiangming Wen

Abstract—Coordinated multipoint (CoMP) is corroborated to be an effective technology in mitigating cochannel interference (CCI) and enhancing system performance in picocell systems, which consist of a large number of pico base stations (BSs). In picocell systems, effective CoMP clustering schemes could provide significant gains of system performance such as throughput and cell-edge spectrum efficiency (SE). Moreover, an intrinsic problem of densely deployed networks is the cost of signaling overhead and data exchange between BSs in clusters. In this paper, a novel semidynamic clustering scheme based on affinity propagation for CoMP-Pico is presented to maximize user SE and throughput under the constraint of backhaul cost. Our proposed scheme consists of online and offline stages that can achieve good performance and low complexity. Simulation results show that the proposed scheme yields significant gains of SE and throughput and low running time compared with the existing clustering schemes.

Index Terms—Affinity propagation, clustering, coordinated multipoint (CoMP) transmission/reception, picocell, small cell.

I. INTRODUCTION

In heterogeneous small-cell networks (HetSNets), the massive deployment of small base stations (BSs; such as pico BS and femto BS) will cause a serious cochannel interference (CCI) problem [1]. A coordinated multipoint (CoMP) transmission/reception technique is proposed as a key approach to resolving it efficiently. Moreover, CoMP, together with HetSNets, can improve the system coverage and user spectrum efficiency (SE) in Long-Term Evolution Advanced [2]. There are four different scenarios considered for CoMP, including joint transmission, dynamic point selection, dynamic point blanking, and coordinated scheduling/beamforming [3]. In this paper, we will focus on joint

Manuscript received October 27, 2013; revised July 25, 2014; accepted September 29, 2014. Date of publication October 8, 2014; date of current version September 15, 2015. This work was supported in part by the Co-building Project of the Beijing Municipal Education Commission "G-RAN-based Experimental Platform for Future Mobile Communications"; by the National Natural Science Foundation of China under Grant 61101109, Grant 61471025, and Grant 61371079; by the Fundamental Research Funds for the Central Universities under Grant ZY1426; by the Interdisciplinary Research Project in Beijing University of Chemical Technology; and by the China-Postdoctoral-Science-Foundation-funded project.

H. Zhang is with the College of Information Science and Technology, Beijing University of Chemical Technology, Beijing 100029, China (e-mail: dr.haijun.zhang@ieee.org).

H. Liu and X. Wen are with the School of Information and Communications Engineering, Beijing University of Posts and Telecommunications, Beijing 100876, China, and also with the Beijing Key Laboratory of Network System Architecture and Convergence, Beijing University of Posts and Telecommunications, Beijing 100876, China (e-mail: kathy66hui@bupt.edu.cn; xiangmw@bupt.edu.cn).

C. Jiang is with the Department of Electronic Engineering, Tsinghua University, Beijing 100084, China (e-mail: chx.jiang@gmail.com).

X. Chu is with the Department of Electronic and Electrical Engineering, The University of Sheffield, Sheffield S1 3JD, U.K. (e-mail: x.chu@sheffield.ac.uk).

A. Nallanathan is with the Department of Informatics, King's College London, London WC2R 2LS, U.K. (e-mail: nallanathan@ieec.org).

Color versions of one or more of the figures in this paper are available online at <http://ieeexplore.ieee.org>.

Digital Object Identifier 10.1109/TVT.2014.2361931

transmission, where several BSs form a coordination BS cluster (CBC) to jointly serve the users, where a proper scheduling scheme could mitigate CCI.

The BSs in a CBC are connected via high-capacity backhaul links on which complex signaling and user data are exchanged. To reduce the backhaul overhead, some clustering schemes for CBC have been proposed in the literature. The existing clustering strategies could be classified into three categories: static clustering, fully-dynamic clustering, and semidynamic clustering. In [4], Marsch and Fettweis proposed a static clustering algorithm wherein major portions of CoMP gains can be obtained with minimal signaling overhead between clusters. Although the static scheme is simple, the fixed size of clusters might cause unnecessary joint processing. Moreover, the static scheme is simple to operate but is feeble to handle the different degrees of interferences and can only provide limited throughput gain. In this sense, dynamic clustering algorithms are more flexible and practical [5]–[7]. In [7], a fully-dynamic clustering algorithm was presented for a multiuser distributed antenna system to maximize system capacity with low implementation complexity assuming perfect channel state information (CSI). In [8], Papadogiannis *et al.* utilized another dynamic greedy algorithm in the formation of CBCs for multicell cooperative processing. The proposed dynamic greedy algorithm can achieve significant sum rate gains, while enhancing the fairness of the system. Although fully-dynamic clustering schemes can mitigate CCI dynamically, the large signaling flow and time consumption in dense HetSNets could not be ignored. That is, a fully-dynamic scheme can achieve optimal performance but needs exhaustive information interchange, which will bring more complexity. Considering the tradeoff between performance and complexity, our semidynamic clustering scheme aims at reducing the complexity without much loss of performance.

The affinity propagation was first proposed by Frey and Duech in 2007 [9], originally, to cluster images of faces, detect genes in microarray data, and identify a representative sentence. It was later extended to the clustering of vehicle ad hoc networks [10] and cognitive radio networks [11]. It has been demonstrated that an affinity propagation algorithm has fast convergence and good performance even with limited prior information [12], [13]. Hence, only partial CSI is needed when an affinity propagation algorithm is applied in wireless communications. In picocell CoMP, pico BSs are usually densely deployed, where complete CSI is hardly available. The affinity propagation algorithm fits perfectly in this scenario, because of its high clustering quality with limited CSI and an efficient convergence rate. However, affinity propagation has been rarely used in CoMP picocells. In [13], Wesemann and Fettweis presented a decentralized BS clustering scheme based on affinity propagation.

In this paper, we propose a semidynamic clustering framework consisting of offline and online stages to maximize the SE and throughput with low signaling overhead in densely deployed CoMP-enabled picocells. The measurement BS cluster (MBC) for CoMP is decided based on geographical locations and the reference signal received power (RSRP) at the offline stage; then, at the online stage, we propose a clustering algorithm to choose CBC from MBC based on limited CSI. Moreover, the affinity propagation principle is used at the online stage to guide the proposed affinity-propagation-based online clustering (APOnC) algorithm. The proposed scheme is proved to be effective and only needs limited CSI between local and neighboring cells, compared with existing static and fully-dynamic clustering schemes.

The rest of this paper is organized as follows. We introduce the basic framework of CoMP in Section II. Then, we present the procedures of the semidynamic clustering scheme and propose our APOnC algorithm in Section III. In Section IV, the performance of the proposed algorithms is evaluated by simulations. Finally, Section V summarizes this paper.

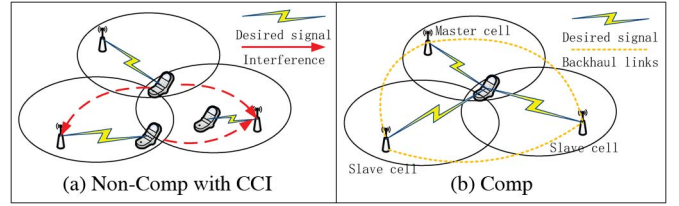


Fig. 1. CoMP and non-CoMP system.

II. BASIC CoMP FRAMEWORK

In this paper, the downlink of a cellular network with B hexagonal cells using the uplink feedback is considered. Let U_b denote the user set served within the coverage of picocell b , $\forall b \in \{1, 2, \dots, B\}$. Each user has a single transmit antenna, and each BS has n_r receive antennas. In our model, a round-robin (RR) scheduling scheme is applied, and the multiple-input multiple-output (MIMO) channel is assumed to be flat fading.

A. Non-CoMP MIMO System

The single-user MIMO (SU-MIMO) scheme is applied in the non-CoMP MIMO system shown in Fig. 1(a). CCI affects the user performance particularly when a user equipment (UE) device locates at the edge of its serving cell. The received signal at user k served by BS b ($k \in U_b$) is given by

$$y_{\text{non}} = \underbrace{h_k^b s_k^b}_{\text{desired signal}} + \underbrace{\sum_{j \in U_{b'}} h_j^{b'} s_j^{b'}}_{\text{interference signal}} + n_k^b \quad (1)$$

where s_k^b and $s_j^{b'}$ are the symbols transmitted by the desired UE k and interfering UE j occupying the same resource block (RB), respectively, the variance of transmitted symbol s_k^b is $E\{|s_k^b|^2\} = p_k^b \geq 0$, h_k^b is the channel gain from UE k to BS b , and n_k^b denotes the additive white Gaussian noise with zero mean and variance $E\{|n_k^b|^2\} = \sigma^2$.

Hence, the non-CoMP signal-to-interference-plus-noise ratio (SINR) for user k served by BS b is

$$\text{SINR}_{\text{non}} = \frac{|h_k^b|^2 p_k^b}{\sigma^2 + \sum_{k \neq j, j \notin U_b} |h_j^b|^2 p_j^b}. \quad (2)$$

Based on Shannon's capacity formula, the achievable capacity of non-CoMP user k served by BS b is given by

$$C_{\text{non}} = BW \log_2(1 + \text{SINR}_{\text{non}}) \quad (3)$$

where BW is the bandwidth of each subchannel.

B. CoMP MIMO System

In CoMP joint transmission, several BSs constructing a CBC jointly transmit data to the CoMP user, as shown in Fig. 1(b). Joint transmission at the BS side enables the mitigation of intracluster CCI and improves throughput particularly for cell-edge users. A central unit (CU) controls signals and data flow. To simplify the analysis, one of the BSs in a CBC is chosen to be the CU and is called the master BS, and other BSs act as slave BSs. All BSs inside a CBC are connected with each other by fibers.

Let \mathbf{W}^C be the zero-forcing combining weight matrix at the UE devices' receiver and u be the single CoMP user in cluster C , then the

signal after joint reception is given by

$$\tilde{\mathbf{Y}}_{\text{CoMP}} = \underbrace{\mathbf{W}^C \mathbf{H}_u^C \mathbf{S}_u^C}_{\text{desired signal}} + \underbrace{\sum_{j \in U_{b'}, b' \in C'} \mathbf{W}^C \mathbf{H}_j^{C'} \mathbf{S}_j^{C'}}_{\text{intercluster interference}} + \mathbf{W}^C n_k^C \quad (4)$$

where \mathbf{H}_u^C is the channel gain matrix from UE u to BSs in cluster C ; \mathbf{S}_u^C and $\mathbf{S}_j^{C'}$ are the symbol matrices transmitted by the desired UE u and interfering UE j occupying the same RB, respectively; and the second term on the right-hand side indicates the interference from users in neighboring clusters.

The CoMP SINR for user k in cluster C is

$$\text{SINR}_{\text{CoMP}} = \frac{|h_k^b|^2 p_k^b}{|\sigma|^2 + \sum_{j \in U_{C'}, C' \neq C} |h_j^b|^2 p_j^b}. \quad (5)$$

Based on Shannon's capacity formula, the achievable capacity of CoMP user k served by BS b is given by

$$C_{\text{CoMP}} = BW \log_2(1 + \text{SINR}_{\text{CoMP}}). \quad (6)$$

C. Pair CoMP SINR Gain

Here, we set a CBC C consisting of BS b and BS b' , and let b act as the master BS. UE devices k and m belong to BSs b and b' , respectively. The CoMP strategy can eliminate CCI from user m to user k . We define a variable to measure the desire of BS b to cooperate with BS b' , $pcg(b, b')$, which is called the pair CoMP SINR gain and is given by

$$\begin{aligned} pcg(b, b') &= \frac{\text{SINR}_{\text{CoMP}}}{\text{SINR}_{\text{non}}} = \frac{\frac{|w_k h_k^b|^2 p_k^b}{|w_k \sigma|^2 + \sum_{j \in U_{C'}} |w_k h_j^b|^2 p_j^b}}{\frac{|h_k^b|^2 p_k^b}{\sigma^2 + \sum_{j \in U_{C'}} |h_j^b|^2 p_j^b + h_m^b p_m^b}} \\ &= \frac{|w_k h_k^b|^2 \left[\sigma^2 + \sum_{j \in U_{C'}} |h_j^b|^2 p_j^b + h_m^b p_m^b \right]}{|w_k h_k^b|^2 \left[\sigma^2 + \sum_{j \in U_{C'}} |h_j^b|^2 p_j^b \right]} \\ &= 1 + \frac{h_m^b p_m^b}{\sigma^2 + \sum_{j \in U_{C'}} |h_j^b|^2 p_j^b}. \end{aligned} \quad (7)$$

III. PROPOSED ADAPTIVE CLUSTERING SCHEME

A. Adaptive Semidynamic Clustering Scheme

Here, two kinds of BS clusters are involved: MBC and CBC. *MBC* denotes the set of BSs that share measurement information such as power levels and CSI, whereas *CBC* denotes the set of BSs that jointly receive and process data from the CoMP user. MBC is identical to CBC in a static clustering strategy and is fixed by the network, whereas in fully-dynamic and semidynamic schemes, the CBC is a subset of MBC. In Fig. 2, we decompose the semidynamic clustering scheme into two stages: The offline stage identifies the MBC based on geographical location and RSRP, whereas the online stage chooses the CBC from MBC. The detailed procedure is described below.

Offline Stage: In realistic systems, only a limited number of BSs can cooperate because of affordable communication overhead [8]. Hence, we set the MBC to include a central BS and six neighboring BSs that

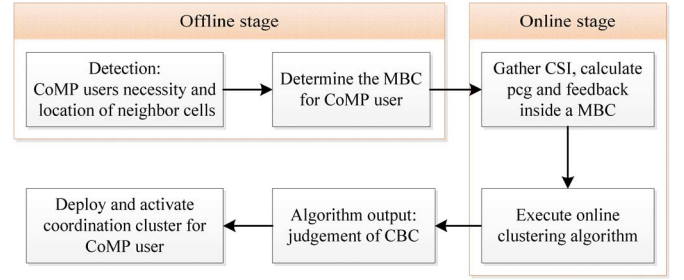


Fig. 2. Framework of CoMP system.

surround it. The CoMP user sends CoMP request to the central serving BS, and then, the network launches the offline stage and forms an MBC for the user based on geographical locations of BSs and RSRP.

Online Stage: In an MBC for each user, CSI for example, CoMP-pair SINRs of sounding reference signal (SRS) can be evaluated and feed back to BSs periodically. By analyzing them according to some criterion, we can select the CBC for the certain CoMP user. A lower SINR_{SRS} means that the user suffers greater interference and needs more coordinating BSs to serve it. Furthermore, the clustering criterion takes SINR_{SRS} and backhaul overhead cost into consideration.

B. Proposed APOnC Algorithm

In the proposed APOnC algorithm, we introduce a concept called “exemplar,” an input key variable called “similarity,” and two information variables called “responsibility” and “availability.” The exemplar for BS i represents the master BS of the cluster including BS i .

The *similarity* $s(i, k)$ indicates how well BS k is suited to be the exemplar for BS i . In particular, $s(k, k)$ is referred to as “preference,” and BSs with larger *preference* values are more likely to be chosen as exemplar BSs. The *similarity* matrix is the unique input of the APOnC algorithm and has a direct impact on the performance. Through the analysis of the online stage, we define the nondiagonal elements of the *similarity* matrix based on *pcg* described in Section II-C. The BS with lower SINR_{non} is more likely to be an exemplar. Nevertheless, more cooperation means more signaling and data exchange cost. Hence, a negative variable c is introduced to indicate the cost. Therefore, we define $s(i, k)$ as follows:

$$s(i, k) = \begin{cases} \log(pcg(i, k)), & i \neq k \\ \beta \cdot \left[\log\left(\frac{1}{\text{SINR}_{\text{non}}^i}\right) - c \right], & i = k \end{cases} \quad (8)$$

where β is a coordinative parameter to adjust the size of clusters, c is the indicator of signaling and data exchange cost, and $\beta \cdot [\log(1/\text{SINR}_{\text{non}}^i) - c]$ defines the *preference*. BSs with lower SINR_{non} have larger *preference* values and are more likely to be chosen as exemplar BSs.

The *responsibility* $r(i, k)$ is sent from BS i to candidate exemplar BS k , as shown in Fig. 3(a). $r(i, k)$ reflects the accumulated evidence of how well suited BS k is to serve as the exemplar BS for BS i , taking into consideration other potential exemplars for BS i . Each BS updates *responsibility* following the rule:

$$r(i, k) = s(i, k) - \max_{\substack{k' \neq k \\ k' \in \text{adj}(i)}} \{a(i, k') + s(i, k')\} \quad (9)$$

where $a(i, k')$ is the *availability* sent from candidate exemplar BS k' to BS i , as shown in Fig. 3(b). $a(i, k)$ reflects the accumulated evidence for how appropriate it would be for BS i to choose BS k as its

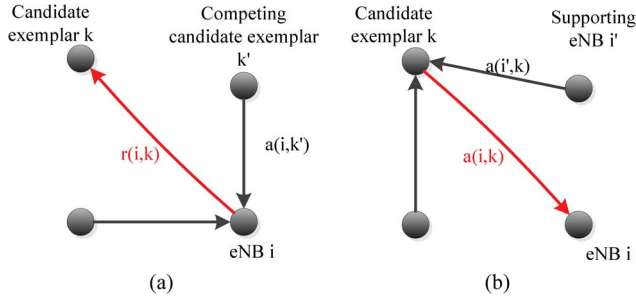


Fig. 3. Schematic of *responsibility* and *availability*. (a) Sending responsibilities. (b) Sending availabilities.

exemplar. Each BS updates *availability* and *self-availability* following the rules:

$$\begin{aligned}
 a(i, k) &= \min \left(0, r(k, k) + \sum_{\substack{i' \notin \{i, k\} \\ i' \in \text{adj}(k)}} \max \{0, r(i', k)\} \right) \\
 a(k, k) &= \sum_{\substack{i' \neq k \\ i' \in \text{adj}(k)}} \max \{0, r(i', k)\}.
 \end{aligned} \quad (10)$$

C. Algorithm Flow

The proposed semidynamic clustering scheme with the APOnC algorithm consists of three major steps: Step A is for MBC initialization in the offline stage; step B is online information broadcasting, where *ITER* is the maximal iteration of *iter*; and step C is the selection of CBC.

Algorithm 1 Semidynamic clustering scheme with APOnC algorithm.

Input:

The set of BSs, $\mathbf{N} = \{1, 2, \dots, N\}$;

The set of UE devices, $\mathbf{U}_{\text{CoMP}} = \{1, 2, \dots, U_{\text{CoMP}}\}$ and $\mathbf{U}_{\text{Non}} = \{1, 2, \dots, U_{\text{non}}\}$;

Output:

Ensemble of CBCs, $\mathbf{C} = \{C_1, C_2, \dots, C_U\}$;

A) Initialization:

- 1: Determine MBC for each user in the offline stage;
- 2: Calculate *similarity* matrix \mathbf{S} according to (8);
- 3: Set initial *availability* matrix $\mathbf{A} = [\mathbf{0}]_{N \times N}$, *responsibility* matrix $\mathbf{R} = [\mathbf{0}]_{N \times N}$ for each user;

B) Iteration:

- 4: **repeat**
- 5: a) Update *responsibility* $\mathbf{R}(i, :)$ by (9) and broadcast;
- 6: b) Update *availability* $\mathbf{A}(:, k)$ by (10) and broadcast;
- 7: Oscillatory decay: (α and $\zeta \in [0, 1]$)
- 8: $\mathbf{R}(\text{iter}) = \alpha \cdot \mathbf{R}(\text{iter}) + (1 - \alpha) \cdot \mathbf{R}(\text{iter} - 1)$,
- 9: $\mathbf{A}(\text{iter}) = \zeta \cdot \mathbf{A}(\text{iter}) + (1 - \zeta) \cdot \mathbf{A}(\text{iter} - 1)$,
- 10: **until** Convergence or *iter* = *ITER*

C) Exemplar judgment:

- 11: **for** *ibs* = 1 to *N* **do**
 - 12: *exemplar* (*ibs*) = $\arg \max_{k \in \text{adj}(\text{ibs})} \{a(\text{ibs}, k) + r(\text{ibs}, k)\}$
 - 13: **end for**
-

The proposed algorithm can be implemented in each cluster using only local information and limited CSI between neighboring cells, where the CSI can be exchanged via backhaul links.

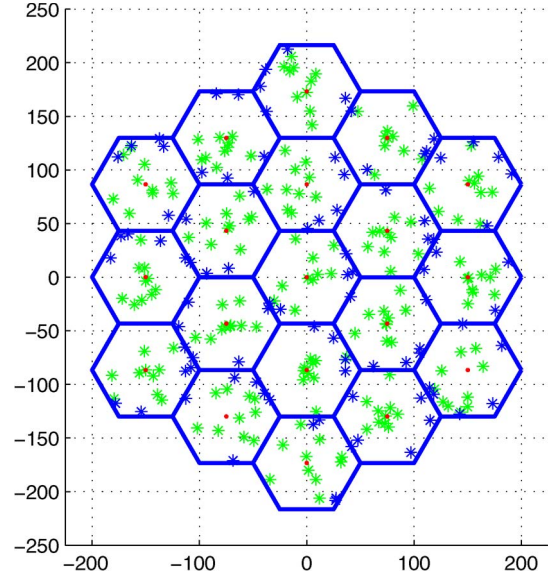


Fig. 4. System model of small cells and users.

The complexity of the affinity propagation algorithm in terms of running time depends on the number of iterations. If there are n samples and there are n^2 values in responsibility matrix R , then updating responsibility $r(i, j)$ requires $O(n - 1)$, and updating availability $a(i, j)$ takes $O(n - 2)$ for each value. As a result, each iteration requires $O(2 * n^3 - 3 * n^2) = O(n^3)$.

The convergence of the affinity propagation algorithm has been proven in [12] and [13], which can guarantee the practicality of the proposed Algorithm 1.

IV. SIMULATION RESULTS

A dense HetSNet consisting of 19 small BSs (picocell BSs) is simulated, as shown in Fig. 4. The channel model based on a 3GPP TR 25.996 urban micro scenario includes shadow fading, large-scale path loss, and multipath fading. The values of β and heuristic cost parameter c are 0.3 and 1 in the simulation determined by a “trial and error” method, respectively. Both values of α and ζ in lines 8 and 9 of Algorithm 1 is 0.8. We assume that the distance between two adjacent BSs is 50 m and that there are 15 uniformly distributed UE devices within each cell. An RR scheduler is employed in each BS. For further performance analysis, we classify all UE devices into central and edge UE devices based on the distance between the UE and its serving BS. As shown in Fig. 4, the red points denote the small-cell BSs, and the green and blue points denote central and edge users, respectively.

The simulation results are given in terms of a UE SE cumulative distribution function (cdf) to indicate system gain and estimated signaling and data cost based on the size of CBC to indicate backhaul cost.

A non-CoMP scheme and two CoMP clustering schemes are also evaluated for comparison with our proposed scheme.

- 1) **Non-CoMP:** In this scheme, each user transmits to its serving BS, while it will cause CCI to its neighboring cells.
- 2) **Static CoMP clustering scheme (static-CoMP):** In this scheme, cluster formulation is fixed, and the MBC is equal to the CBC. Three adjacent BSs are grouped into one CBC for a CoMP user.
- 3) **Signal-interference matrix (SIM)-based CoMP clustering scheme (SIM-CoMP) [7]:** In this scheme, MBC for the CoMP user includes the serving BS and its neighboring BSs at the offline stage. The user compares the ratio of the biggest interference component and the signal component with a threshold. The online clustering of CBC depends on the ratio.

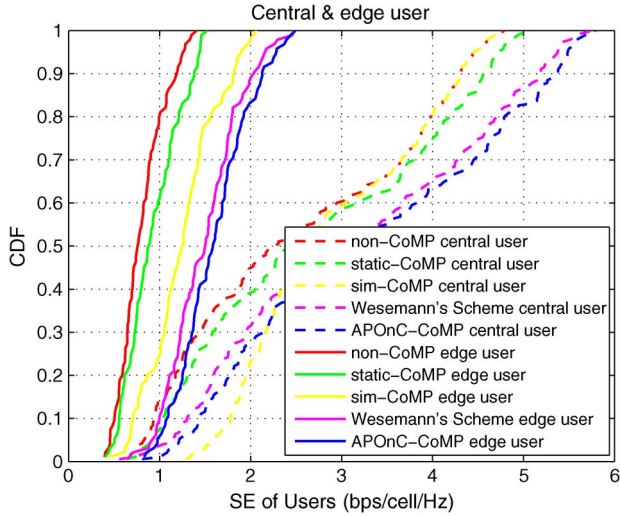


Fig. 5. CDF of central and edge users, where SE is calculated using (C_{non}/BW) or (C_{CoMP}/BW) .

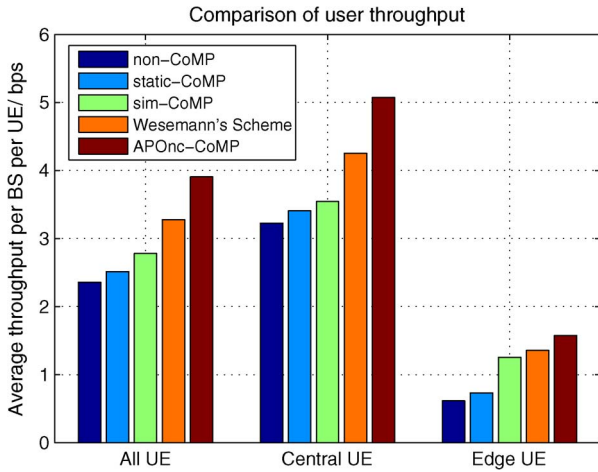


Fig. 6. Average user throughput of different clustering schemes, where throughput is calculated using (3) or (6).

The SE cdf curves of both central and edge UE devices for each considered scheme are given in Fig. 5. It can be observed that the four CoMP schemes achieve higher SE than the non-CoMP scheme, because CoMP can efficiently combat the intercell interference. Moreover, our proposed clustering scheme provides the best SE for both central and edge users among the four CoMP schemes. With non-CoMP set as the baseline, the throughput gain of CoMP over non-CoMP is more evident for edge users than for central users, particularly with the SIM-CoMP, Wesemann's scheme [13], and APOnC CoMP. The reason is that the edge users suffer from higher CCI and lower SINR; hence, they have more demands and opportunities for coordination. In other words, the CoMP strategy is more effective for enhancing cell-edge performance.

Fig. 6 shows the average throughput of the proposed algorithm and the existing schemes. We can see that CoMP schemes can achieve higher throughput than the non-CoMP system. The throughput gains are much more significant for edge UE devices than for central UE devices, particularly with the SIM-CoMP, Wesemann's scheme [13], and APOnC CoMP. In addition, due to the effective information interchange mechanism, our proposed semidynamic clustering scheme with the APOnC algorithm obtains the highest average throughput among the four CoMP schemes and the largest gain over the non-

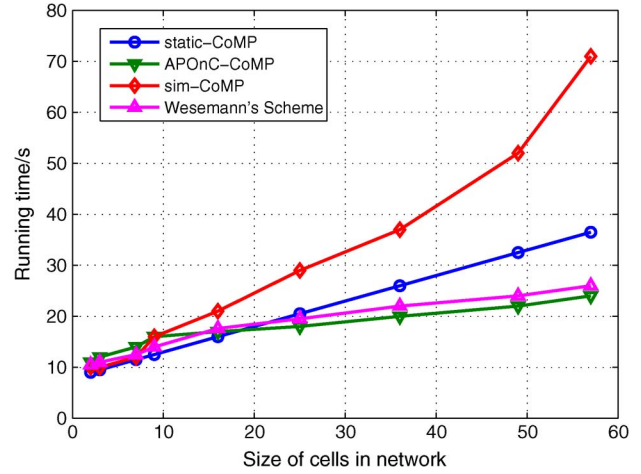


Fig. 7. Running time comparison.

CoMP scheme. In both Figs. 5 and 6, the effectiveness of CoMP schemes compared with non-CoMP can be observed. Moreover, the APOnC CoMP scheme achieves a better performance than the existing CoMP schemes.

In dense small-cell networks, the complexity influences the system performance. Hence, we compare the running time of static-CoMP, SIM-CoMP, Wesemann's scheme, and our scheme in Fig. 7 to evaluate the algorithm complexity. We can see that when the number of BSs increases, the running time of all the four schemes increases. The running time of the APOnC CoMP scheme becomes lowest of the three schemes when the number of picocells goes beyond 19. The APOnC CoMP scheme achieves higher throughput with relatively lower complexity.

V. CONCLUSION

In this paper, we have proposed a semidynamic clustering CoMP scheme for dense small-cell networks to improve user throughput with consideration of backhaul cost and complexity. Our scheme consists of offline and online stages to implement efficient clustering. The MBC for the CoMP users is decided based on geographical locations and RSRP at the offline stage, and then, at the online stage, we propose a novel APOnC algorithm to choose CBC from MBC based on limited CSI. The proposed scheme is proved to be effective and only need limited CSI between local and neighboring cells, compared with existing static and fully-dynamic clustering schemes. The performance of the proposed scheme is evaluated by comparing with some existing schemes in the simulation. The results show that our scheme can increase user SE and cell throughput particularly for edge users. Moreover, our scheme requires reduced complexity as compared with other clustering algorithms, proving to be more practical in dense small-cell systems.

REFERENCES

- [1] D. Lopez-Perez *et al.*, "Enhanced intercell interference coordination challenges in heterogeneous networks," *IEEE Wireless Commun.*, vol. 18, no. 3, pp. 22–30, Jun. 2011.
- [2] J. Lee *et al.*, "Coordinated multipoint transmission and reception in LTE-Advanced systems," *IEEE Commun. Mag.*, vol. 50, no. 11, pp. 44–50, Nov. 2012.
- [3] H. Maattanen *et al.*, "System-level performance of LTE-Advanced with joint transmission and dynamic point selection schemes," *EURASIP J. Adv. Signal Process.*, vol. 2012, no. 1, pp. 247:1–247:18, Nov. 2012.
- [4] P. Marsch and G. Fettweis, "Static clustering for cooperative multi-point (CoMP) in mobile communications," in *Proc. IEEE ICC*, Jun. 2011, pp. 1–6.

- [5] S. Nam, J. Oh, and Y. Han, "A dynamic transmission mode selection scheme for CoMP systems," in *Proc. IEEE PIMRC*, Sep. 2012, pp. 483–487.
- [6] B. Makki, T. Eriksson, and T. Svensson, "On an HARQ-based coordinated multi-point network using dynamic point selection," *EURASIP J. Wireless Commun. Netw.*, vol. 2013, no. 1, p. 209, Aug. 2013.
- [7] X. You *et al.*, "Cooperative distributed antenna systems for mobile communications [Coordinated and Distributed MIMO]," *IEEE Wireless Commun.*, vol. 17, no. 3, pp. 35–43, Jun. 2010.
- [8] A. Papadogiannis, D. Gesbert, and E. Hardouin, "A dynamic clustering approach in wireless networks with multi-cell cooperative processing," in *Proc. IEEE ICC*, 2008, pp. 4033–4037.
- [9] B. J. Frey and D. Dueck, "Clustering by passing messages between data points," *Science*, vol. 315, no. 5814, pp. 972–976, Feb. 2007.
- [10] C. Shea, B. Hassanabadi, and S. Valaee, "Mobility-based clustering in VANETs using affinity propagation," in *Proc. IEEE GLOBECOM*, Dec. 2009, pp. 1–6.
- [11] K. E. Baddour, O. Ureten, and T. J. Willink, "Efficient clustering of cognitive radio networks using affinity propagation," in *Proc. ICCCN*, Aug. 2009, pp. 1–6.
- [12] J. Yu and C. Jia, "Convergence analysis of affinity propagation," in *Knowledge Science, Engineering and Management*. Berlin, Germany: Springer-Verlag, 2009, pp. 54–65.
- [13] S. Wesemann and G. Fettweis, "Decentralized formation of uplink CoMP clusters based on affinity propagation," in *Proc. ISWCS*, Aug. 2012, pp. 850–854.

Training-Based SWIPT: Optimal Power Splitting at the Receiver

Xiangyun Zhou

Abstract—We consider a point-to-point system with simultaneous wireless information and power transfer (SWIPT) over a block-fading channel. Each transmission block consists of a training phase and a data transmission phase. Pilot symbols are transmitted during the training phase for channel estimation at the receiver. To enable SWIPT, the receiver adopts a power-splitting design, such that a portion of the received signal is used for channel estimation or data detection, while the rest is used for energy harvesting. We optimally design the power-splitting ratios for both training and data phases to achieve the best ergodic capacity performance while maintaining a required energy harvesting rate. Our result shows how a power-splitting receiver can make the best use of the received pilot and data signals to obtain optimal SWIPT performance.

Index Terms—Channel estimation, power splitting, simultaneous wireless information and power transfer (SWIPT), training.

I. INTRODUCTION

Recently, the concept of simultaneous wireless information and power transfer (SWIPT) has drawn considerable attention [1]–[11]. With simple circuit designs, the receiver is able not only to decode the information carried by the RF signal but to harvest energy from the same signal as well. Two practical receiver designs that have been

Manuscript received May 13, 2014; revised August 21, 2014; accepted October 9, 2014. Date of publication October 21, 2014; date of current version September 15, 2015. This work was supported by the Australian Research Council's Discovery Projects funding scheme under Project DP140101133. The review of this paper was coordinated by Dr. S. Tomasin.

The author is with the Research School of Engineering, The Australian National University, Acton, ACT 2601, Australia (e-mail: xiangyun.zhou@anu.edu.au).

Color versions of one or more of the figures in this paper are available online at <http://ieeexplore.ieee.org>.

Digital Object Identifier 10.1109/TVT.2014.2364196

widely accepted are *time switching* and *power splitting* [1]. With the time-switching design, e.g., in [2], [8], and [9], the receiver is either in the information decoding mode or the energy harvesting mode at any point in time. For this to happen, new frame structures must be designed to include energy harvesting time slots. On the other hand, the power-splitting design, e.g., in [2], [3], [6], [7], and [9]–[11], enables the receiver to split the received signal into two streams, i.e., one going to the information decoding circuit and the other going to the energy harvesting circuit. When splitting the signal, the power of the signal is also divided. The basic power-splitting design requires no change in the conventional communication systems apart from the receiver circuit.

Current studies on SWIPT systems often assume perfect channel knowledge with a few exceptions, considering imperfect channel knowledge at the transmitter, e.g., [12]. On the other hand, imperfect channel estimation at the receiver has yet to be considered. For communications over time-varying fading channels, pilot symbols are periodically transmitted to facilitate channel estimation at the receiver, and the estimation is never perfect in practice. The tradeoff in resource allocation between channel training and data transmission has been extensively investigated for conventional communication systems with information transfer only [13]–[15]. Some recent independent research has also studied the resource allocation between training and energy transfer in multiantenna systems without considering information transfer [16], [17]. In a SWIPT system, both information and energy transfers are required; hence, how to achieve the best tradeoff in resource allocation between channel estimation, data detection, and energy harvesting has become an interesting open problem. In this paper, we study such a tradeoff by focusing on the power-splitting design at the receiver.

We consider a training-based SWIPT system. Each transmission block starts with a training phase followed by a data transmission phase. Considering a block-fading channel, the system aims to achieve the best ergodic capacity performance while maintaining a target energy harvesting rate. To this end, we optimally design the power-splitting ratios during both training and data phases, which are denoted by ρ_p and ρ_d . Specifically, ρ_p controls the resource allocation between channel estimation and energy harvesting during the training phase, and ρ_d controls the resource allocation between data detection and energy harvesting during the data phase. We propose both nonadaptive and adaptive power-splitting designs. In the nonadaptive design, ρ_p and ρ_d have fixed values for all blocks. In the adaptive design, ρ_p is fixed, whereas ρ_d is dynamically chosen according to the estimated channel gain in each block. The main contributions of this work are summarized as follows.

- One novel aspect of this work is the consideration of power splitting during the training phase. Our result shows that, when the training resource is limited, the receiver should use most, if not all, power for channel estimation during the training phase and leave the burden on energy harvesting to the data phase. The optimal values of ρ_p and ρ_d are generally very different, which implies the importance of having different power-splitting designs for training and data phases.
- The adaptive power-splitting design results in a significantly improved capacity performance, as compared with the nonadaptive design, when the required energy harvesting rate is moderate to large. For the adaptive design, we also analytically compare the optimal values of ρ_d with perfect and imperfect channel estimation and find them to be fundamentally different. For example, one should use all power for energy harvesting when the estimated channel gain is sufficiently small, whereas in the